



## Phytoplankton dynamics in the Gulf of Aqaba (Eilat, Red Sea): A simulation study of mariculture effects



Leonardo Laiolo<sup>a</sup>, Alberto Barausse<sup>b,\*</sup>, Zvy Dubinsky<sup>c</sup>, Luca Palmeri<sup>b</sup>, Stefano Goffredo<sup>a</sup>, Yury Kamenir<sup>c</sup>, Tariq Al-Najjar<sup>d</sup>, David Iluz<sup>c,\*</sup>

<sup>a</sup> Marine Science Group, Department of Biological, Geological and Environmental Sciences, Section of Biology, Alma Mater Studiorum, University of Bologna, Bologna, Italy

<sup>b</sup> Environmental Systems Analysis Lab (LASA), Department of Industrial Engineering, University of Padova, Padova, Italy

<sup>c</sup> The Mina & Everard Goodman Faculty of Life Sciences, Bar-Ilan University, Ramat-Gan, Israel

<sup>d</sup> Marine Science Station, Aqaba, Jordan

### ARTICLE INFO

#### Article history:

Available online 17 July 2014

#### Keywords:

Eilat  
Aqaba  
Phytoplankton dynamics  
Fish farm  
Coastal pollution  
Coral reefs

### ABSTRACT

The northern Gulf of Aqaba is an oligotrophic water body hosting valuable coral reefs. In the Gulf, phytoplankton dynamics are driven by an annual cycle of stratification and mixing. Superimposed on that fairly regular pattern was the establishment of a shallow-water fish-farm initiative that increased gradually until its activity was terminated in June 2008. Nutrient, water temperature, irradiation, phytoplankton data gathered in the area during the years 2007–2009, covering the peak of the fish-farm activity and its cessation, were analyzed by means of statistical analyses and ecological models of phytoplankton dynamics. Two datasets, one from an open water station and one next to the fish farms, were used. Results show that nutrient concentrations and, consequently, phytoplankton abundance and seasonal succession were radically altered by the pollution originating from the fish-farm in the sampling station closer to it, and also that the fish-farm might even have influenced the open water station.

© 2014 Elsevier Ltd. All rights reserved.

### 1. Introduction

Coral reefs are among the most productive and biologically diverse ecosystems on Earth and supply people with goods and services as seafood, recreational possibilities, coastal protection, as well as aesthetic and cultural benefits (Moberg and Folke, 1999). The coral reef off the coast of the cities of Eilat (Israel) and Aqaba (Jordan) stretches over 1200 m along the east and west coasts of the Gulf of Aqaba (Bay of Eilat). This coral reef supports a thriving economy based primarily on tourism. Natural and anthropogenic factors threaten this important source of revenue; in particular, sea-water quality is worsening due to pollution caused by human activities in the coastal zones surrounding the gulf, e.g., metallurgical industries, hotels and resorts, port activities and fish farming (Loya and Kramarsky-Winter, 2003; Loya et al., 2004; Chen et al., 2007, 2008; Lazar et al., 2008). Global climate change may also be a contributory factor: dust is deposited in

the gulf by sand storms due to desertification processes, which favor phytoplankton growth. These processes could be aggravated by water-warming and acidification caused by an anthropogenic increase in atmospheric greenhouse gases, and an increase in UV radiation due to ozone depletion, although it must be stressed that evidences for statistically significant warming or acidification of the Gulf of Aqaba have not been found yet to our knowledge. For their nutrient supply, the productive coral reefs in the Gulf of Aqaba subsist, to a large degree, on allochthonous plankton, providing nitrogen fluxes from the phytoplankton to the coral reef (Yahel et al., 1998; Richter et al., 2001). Therefore, the inter-annual variability in the intensity and timing of phytoplankton blooms, triggered by water-column mixing, and nutrient injections from the fish farm activity, might have serious consequences for the upper trophic levels in the Gulf of Aqaba and its food web, including coral reef stability (Labiosa et al., 2003). Indeed, nutrients excreted by farmed fish can be readily taken up by phytoplankton and stimulate their growth, which can potentially lead to localized eutrophication, especially in coastal areas of poor flushing (Brown et al., 1987; Aure and Stigebrandt, 1990; Wu et al., 1994; Wu 1995). This study investigates the impact of fish-farming activities and their cessation on water quality and phytoplankton dynamics in the Northern Gulf of Aqaba.

\* Corresponding authors. Address: Department of Industrial Engineering, University of Padova, Via Marzolo 9, 35131 Padova, Italy. Fax: +39 049 827 7599 (A. Barausse). Tel.: +972 52 8633069; fax: +972 3 7384058 (D. Iluz).

E-mail addresses: [alberto.barausse@unipd.it](mailto:alberto.barausse@unipd.it) (A. Barausse), [iluzda@mail.biu.ac.il](mailto:iluzda@mail.biu.ac.il) (D. Iluz).

### 1.1. Seasonal phytoplankton dynamics in the northern Gulf of Aqaba

The Gulf of Aqaba is characterized by seasonal cycles of stratification and mixing, similar to other subtropical oligotrophic seas. Small perturbations, such as transient cooling, which induces convection, and wind events driving upwelling can, at times, inject deep water into the euphotic layer, making nutrients available for phytoplankton growth (Labiosa et al., 2003). The water column of the northern Gulf of Aqaba is stratified during summer and, under usual conditions, surface water nutrient levels are depleted to levels near the limits of detection (Levanon-Spanier et al., 1979; Mackey et al., 2007). During the summer months, dry atmospheric deposition is a significant source of nutrients in the euphotic zone, supporting transient phytoplankton blooms (Chen et al., 2007; Paytan et al., 2009). Beginning in the fall, the cooling of surface waters initiates a convective mixing along with the erosion of the thermocline, and a deeply (usually 300 m, occasionally down to the bottom) mixed water body is observed by winter (Wolf-Vecht et al., 1992). In summer and fall, when nutrient concentrations are very low, picophytoplankton (cells < 2  $\mu\text{m}$ ) (*Prochlorococcus* and *Synechococcus*) abound in the surface water; with *Prochlorococcus* as the main component of the community during aestival stratification (Lindell and Post, 1995; Post et al., 1996; Mackey et al., 2007). During summer, *Prochlorococcus* and *Synechococcus* populations in the Gulf of Aqaba are exposed to phosphate limitation (Fuller et al., 2005; Mackey et al., 2009). During winter and early spring, the convective component of entrainment is strong enough to mix the surface waters below the critical depth, as well as bring to the surface (Labiosa et al., 2003) large quantities of nutrients, which maintain the nitrogen-phosphorus ratio close to the Redfield ratio (Häse et al., 2006). The increase in nutrient availability following autumnal mixing leads to the replacement of picophytoplankton with larger *Chlorophyceae* and *Cryptophyceae* (Al-Najjar et al., 2007). Indeed, phytoplankton patterns follow the seasonal hydrological cycle in the Gulf of Aqaba (Iluz et al., 2008).

### 1.2. Aim of the study

The aim of this study was to develop ecological models, based on a three-year (2007–2009) dataset, to analyze, simulate, and predict the phytoplankton dynamics in the surface layer (1 m depth) of the northern Gulf of Aqaba. The purpose is to clarify the role of the fish farm activity in a possible alteration of phytoplankton dynamics.

## 2. Materials and methods

### 2.1. Site description

The Gulf of Aqaba is one of two large gulfs in the Red Sea (Fig. 1), located east of the Sinai Peninsula and west of the Arabian mainland, and separated from the Red Sea by the 252-m-deep sill at the Straits of Tiran. This gulf is 170 km long and 14–24 km wide, with an average depth of 800 m and a maximum of 1830 m. For these reasons, the Gulf of Aqaba represents a small-scale, easy-to-access, regional analogue of larger oceanic oligotrophic systems (Chen et al., 2008). In the Gulf of Aqaba, the climate is extremely arid – the annual precipitation at the northern gulf averages only 30 mm – and hot, with summer air temperature reaching up to 45 °C and with prevailing northerly winds. Excess evaporation over this minimal precipitation is in the range of 2000 mm yr<sup>-1</sup> (Monismith et al., 2006). No rivers flow into the gulf, and fresh water, other than rain, reaches it only occasionally during rare winter floods. The coral reef off the coast of Eilat and Aqaba, the two largest cities in this area, supports a thriving economy based primarily on tourism. Relative isolation from the main Red Sea

and the Indian Ocean, intense solar radiation for most of the year, low plankton biomass and levels of particulate organic matter in the water column, characterize the Gulf of Aqaba. The low levels of nitrogen and phosphate are the main factors limiting primary production (Al-Qutob et al., 2002; Labiosa et al., 2003). This area is dominated by mineral dust deposition and is surrounded by deserts; anthropogenic air emissions can make a significant contribution to the level of various trace elements, such as Cu, Cd, Ni and Zn (Chen et al., 2008). In recent years, the atmospheric inputs of other nutrients gradually increased the likelihood of P limitation in the gulf (Chen et al., 2007). Consequently, P limitation in the ocean may be more prevalent than previously estimated, and the efficiency of P uptake among individual groups of phytoplankton may, in fact, control the phytoplankton species composition observed in a given community (Paytan and McLaughlin, 2007).

### 2.2. Sample collection

In this study, a monitoring database from two different sampling stations, the fish-farm station, situated several 100 m off the northern coast of the Gulf of Eilat (FFS, 29°32' N, 34°56' E), and Station A, on the Israeli/Jordanian/Egyptian border (STA, 29°28'N, 34°55'E) (Fig. 1), was used. The data were sampled over a period of three years (from January 14th, 2007, to December 28th, 2009) as part of the project “Protecting the Gulf of Aqaba from Anthropogenic and Natural Stress”, supported by the NATO Science for Peace and Security Program (SPS), aboard the Queen of Sheba research vessel. Data were sampled during monthly cruises, for a total of 35 samplings, including measurements of chemical, physical, and biological parameters at the same depths. In particular, the concentration of chlorophyll *a*, nitrate (NO<sub>3</sub>), phosphate (PO<sub>4</sub>) and silicate (SiOH<sub>4</sub>) as well as water temperature were sampled for both sampling stations at 1 m depth (Fig. 2 A–E). The concentration of nitrite (NO<sub>2</sub>) and ammonium (NH<sub>4</sub><sup>+</sup>) were also sampled but they were not used because they were excessively discontinuous (i.e., contained many gaps). In this work, we chose not to use the irradiance measurements from the sampling stations and, instead, we obtained them from the Interuniversity Institute for Marine Sciences (IUI), Eilat, where hourly observations of irradiance were available, thus providing our study with a dataset characterized by a much higher time resolution (Fig. 2F).

The fish farms were operational until June 17th, 2008 (final closure date), about halfway through the overall sampling period. The maximum sea depth at the FFS location was 56 m. The STA sampling point was about 13 km away from the FFS, had a 700 m maximum depth, and no apparent direct anthropogenic influence, thus representing a sort of control station with respect to the FFS location, which could be expected to be under the potential influence of human coastal processes, such as maricultural activities. To collect the water samples, a CTD-Rosette (Sea-Bird) equipped with 11 Teflon-coated Niskin bottles (12 L), a CTD (SBE 19-02, SeaBird), a photometer, LICOR (Li-190SA), and a fluorometer (Sea-Point Sensors Inc.), were used. Chlorophyll *a* samples (250 ml) were kept in a dark container and processed within 8 h of sampling, concentrated on 25 mm Whatman GF/F filters, extracted overnight in 90% acetone and measured using the fluorometric method described by Parsons et al. (1984). Extracted chlorophyll *a* measurements were used to calibrate the in situ fluorescence profiles measured during the same hydrocast. The CTD fluorescence profiles for hydrocasts with no extracted chlorophyll *a* were calibrated using extracted chlorophyll *a* data from the closest sampling dates. Colorimetric analyses (Grasshoff et al., 1999) were conducted using a Flow Injection Autoanalyzer (Lachat Instruments Model QuikChem 8000). The analyses were fully automated and peak areas were calibrated using standards prepared in nutrient-depleted filtered seawater.

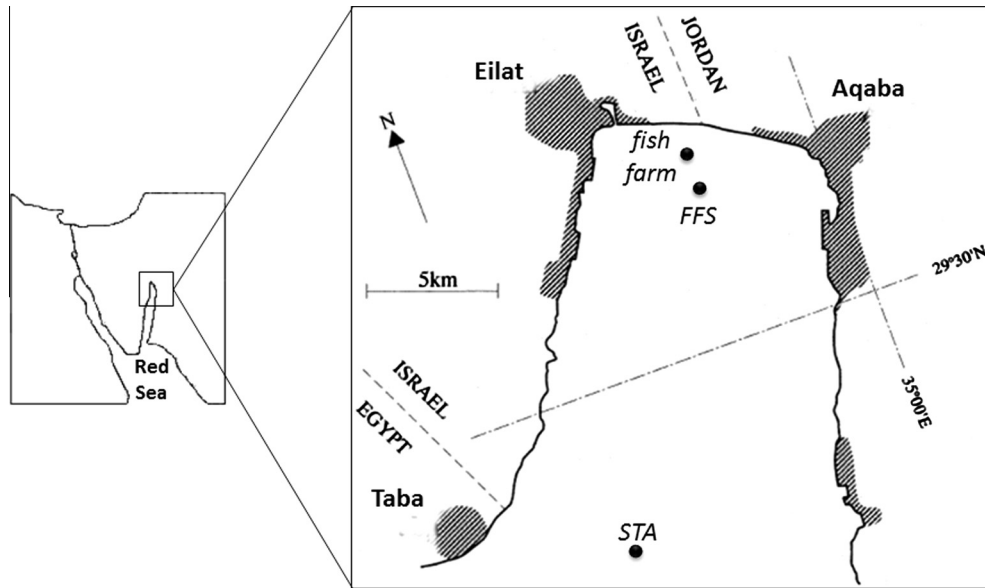


**Fig. 1.** Gulf of Aqaba and sampling points: location of the fish farm and the two sampling points, the fish-farm station (FFS) and Station A (STA) (Lindell and Post, 1995).

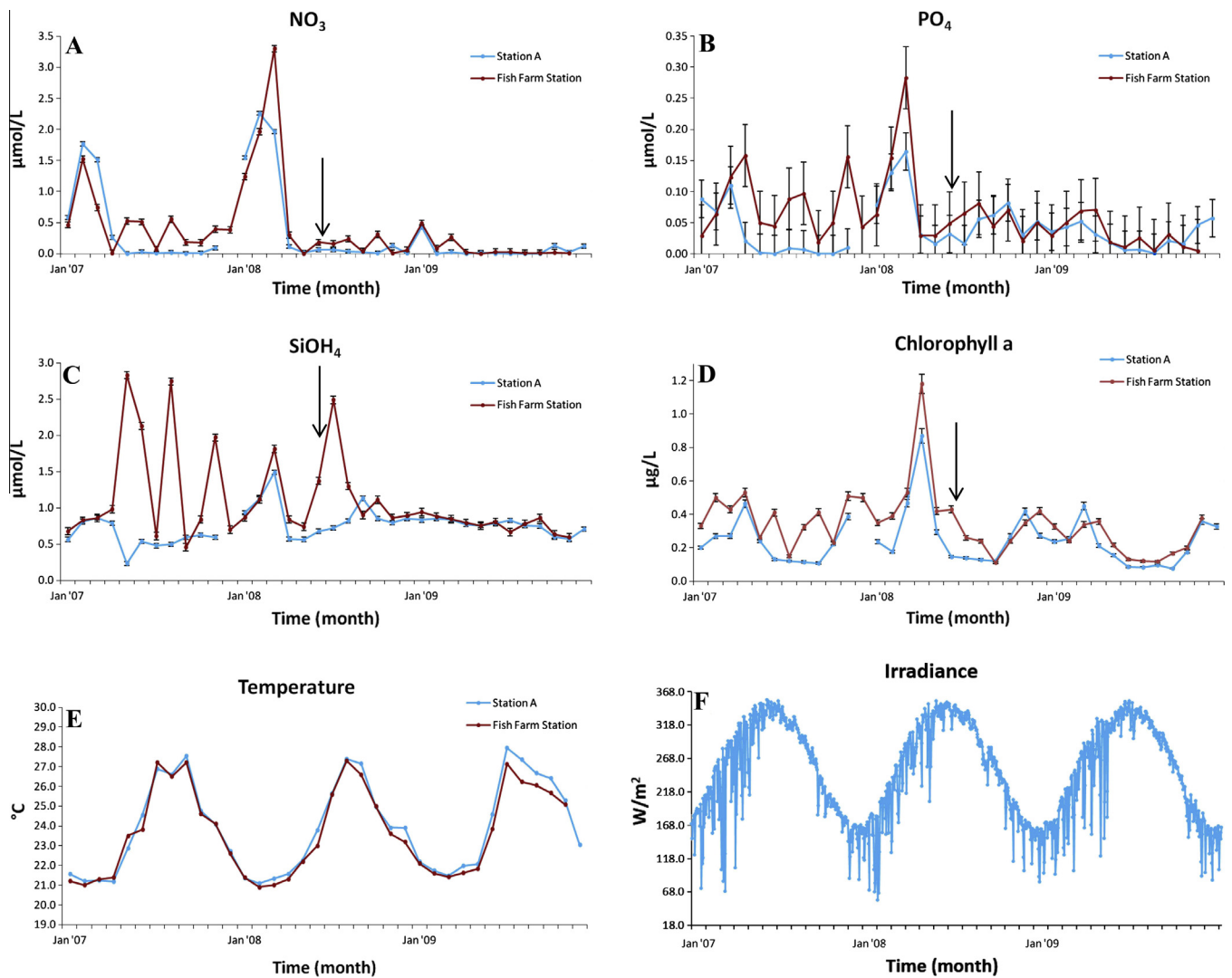


**Fig. 2.** Time series of nutrients, chlorophyll a concentration, temperature, and irradiance: samples were taken at a 1-m depth over the period 2007–2009. The arrows indicate the date of the fish-farm closure. Errors bars (measurement uncertainty) are indicated for  $\text{NO}_3$  ( $\pm 0.05 \mu\text{mol l}^{-1}$ ),  $\text{PO}_4$  ( $\pm 0.03 \mu\text{mol l}^{-1}$ ),  $\text{SiOH}_4$  ( $\pm 0.05 \mu\text{mol l}^{-1}$ ) and chlorophyll a ( $\pm 5\% \mu\text{g l}^{-1}$ ). The irradiance data were collected from the Interuniversity Institute for Marine Sciences (IUI), Eilat.

### 2.3. Statistical analysis

The time series of sampled nutrients and chlorophyll *a* concentration described in the previous section were inspected visually and, then, statistical tests were performed to understand if there were significant differences in concentration between the two sampling stations, in the periods before or after the fish-farm closure. Statistical tests were also performed separately for each sampling station to check if there were significant differences in concentration before and after the fish farm closure. These tests were carried out in each sampling station for chlorophyll *a*, PO<sub>4</sub>, NO<sub>3</sub>, and SiOH<sub>4</sub>. Since data were not normally distributed according to the Shapiro–Wilk *W* test (Shapiro et al., 1968), the non-parametric Mann–Whitney *U* test (Mann and Whitney, 1947) was used to assess whether the concentration of a given sampled substance (chlorophyll *a*, NO<sub>3</sub>, PO<sub>4</sub>, or SiOH<sub>4</sub>) in the period preceding the closure of the fish farm differed from its concentration after the closure, either at the FFS or at the STA site; furthermore, the non-parametric Wilcoxon matched-pairs test (Siegel and Castellan, 1988) was used to investigate whether the concentration of a given sampled substance differed between the STA and the FFS either in the period before or following the stop of fish-farm activities. Multiple comparisons were thus carried out and they were corrected for by applying the Benjamini–Hochberg procedure (Benjamini and Hochberg, 1995; Verhoeven et al., 2005).

### 2.4. Model construction and confrontation

The outcome of the statistical analyses was used to inform the construction of conceptual models of phytoplankton dynamics, each reflecting different but plausible and biologically-sound assumptions regarding the processes driving phytoplankton abundance. Then, such conceptual models were translated into mathematical form by constructing a number of ecological models, which were used to identify the combination of ecological processes best able to describe the dynamics of phytoplankton populations. This was done through a model confrontation (Hilborn and Mangel, 1997; Burnham and Anderson, 2002): each model was run and fitted to chlorophyll *a* observations, and its fit performance was compared to those of the other models to understand which processes better predict phytoplankton dynamics.

In our ecological models, the chlorophyll *a* concentration was chosen as the state variable used to describe phytoplankton dynamics. Several external forcing functions influencing the state variable were included in the models (Table 1): nutrients, light

and water temperature. The maximum growth rate of phytoplankton was assumed to be limited by temperature, nutrient concentrations and light available for the photosynthesis process, and the following widely tested, classic equation that describes the algal growth was chosen to simulate the dynamics of phytoplankton over time (Jørgensen and Bendoricchio, 2001):

$$\frac{dA}{dt} = (\mu - G) \cdot A, \quad (1)$$

Here,  $\frac{dA}{dt}$  represents the change over time of algal biomass *A*, as expressed by chlorophyll *a* concentration,  $\mu$  is the gross growth rate (d<sup>−1</sup>) and *G* (d<sup>−1</sup>) is a lumped, temperature-dependent loss parameter which represents the effect of processes such as respiration, exudation, non-predatory mortality, settling and grazing. The growth rate  $\mu$  was modeled as (Jørgensen and Bendoricchio, 2001):

$$\mu = \mu_{\max}(T_{\text{ref}}) \cdot f[f_1(T) \cdot f_2(L) \cdot f_3(N)] \quad (2)$$

This equation represents a classic, general, and simple method for simulating phytoplankton dynamics (Jørgensen and Bendoricchio, 2001). In this equation,  $\mu_{\max}(T_{\text{ref}})$  is the maximum growth rate attainable at a reference temperature  $T_{\text{ref}}$ , whereas  $f = f_1 \cdot f_2 \cdot f_3$  is a function expressing the limitation imposed on this maximum rate by environmental conditions. A growth value equal to  $\mu_{\max}(T_{\text{ref}})$  is achieved under optimal, non-limiting conditions, with full availability of nutrients and optimal light and temperature levels. Functions  $f_1(T)$ ,  $f_2(L)$ , and  $f_3(N)$  represent the effects of temperature, light limitation, and nutrient starvation on the maximum growth rate, respectively. *T* stands for water temperature, *L* for irradiance and *N* for the concentration of a given nutrient. The values of these forcing functions were taken from the sources described in the section “Sample collection” and were linearly interpolated whenever needed to solve Eq. (1) numerically.

Two common variants for  $f_1(T)$  were tried (Jørgensen and Bendoricchio, 2001): the classic Arrhenius exponential model (henceforth referred to as T\_EXP):

$$f_1(T) = \theta^{(T-T_{\text{ref}})} \quad (3)$$

and a skewed distribution peaking at an optimum temperature (henceforth T\_OPT):

$$f_1(T) = e^{\left[-2.3 \left(\frac{T-T_{\text{opt}}}{T_{\text{x}}-T_{\text{opt}}}\right)^2\right]} \quad (4)$$

where *T* is expressed as °C and  $\theta$  is a parameter whose value should approximately range between 1 and 1.05. Higher values of  $\theta$  increase the influence of temperature on the chlorophyll *a* time

**Table 1**  
Forcing functions: the forcing functions used for model simulations, along with their abbreviations, units, and intervals, are reported. The last column reports additional information and abbreviations (used in Tables 3 and 4) concerning the different types of interactions between multiple nutrients that were tested in the models.

Forcing function	Forcing function abbreviations and mathematical equation	Units	Intervals	Notes
Water temperature	T_EXP (Eq. (3)) T_OPT (Eq. (4))	°C	(FFS) 20.9–27.3 (STA) 21.1–27.9	Function inserted in the models using the formulation of Eq. (3) or Eq. (4).
Nutrient	NO <sub>3</sub> (Eq. (8))	Micromol l <sup>−1</sup>	NO <sub>3</sub> : (FFS) 0.004–3.3 (STA) 0.0001–2.257	<b>LIEB</b> : the nutrient that drives the state variable growth is determined through the Liebig's law of the minimum; <b>KVAR</b> : $k_N$ for the nutrient(s) being considered changes after the fish-farm closure;
	PO <sub>4</sub> (Eq. (8))		PO <sub>4</sub> : (FFS) 0.005–0.283 (STA) 0.0016–0.164	<b>SEASON</b> : NO <sub>3</sub> regulates chlorophyll <i>a</i> dynamics in winter and spring, PO <sub>4</sub> in summer and fall;
	SiOH <sub>4</sub> (Eq. (8)) (nutrient/s that regulate phytoplankton dynamics during the simulation)		SiOH <sub>4</sub> : (FFS) 0.457–2.83 (STA) 0.233–1.488	<b>CHN</b> : indicates that the first nutrient regulates chlorophyll <i>a</i> dynamics before the fish-farm closure while the second nutrient regulates dynamics afterwards.
Irradiance	LIGHT_SAT (Eq. (5)) LIGHT_OPT (Eq. (6))	W m <sup>−2</sup>	(FFS) and (STA) 55.25–355.375	Function inserted in the models using the formulation of Eq. (5), (6).



trajectory, e.g., they exacerbate peaks and troughs in phytoplankton biomass;  $T_{ref}$  was taken to be 24 °C (Jørgensen and Bendoricchio, 2001). Here,  $T_x = T_{min}$  if  $T < T_{opt}$ , and  $T_x = T_{max}$  if  $T \geq T_{opt}$ , where  $T_{min}$  is the minimum temperature under which the growth is zero,  $T_{max}$  is the maximum temperature giving non-zero growth, and  $T_{opt}$  is the optimal temperature for growth.

Function  $f_2(L)$  represents limitation due to the scarcity of light  $L$ , which, in this case, was expressed as irradiance ( $W m^{-2}$ ). For this function, two possible formulations were tried (Jørgensen and Bendoricchio, 2001), the Michaelis–Menten equation, which assumes that light has a positive, saturation-like effect on growth (henceforth LIGHT\_SAT):

$$f_2(L) = \frac{L}{k_L + L} \quad (5)$$

and the Steel formulation (a humped, optimum curve) (henceforth LIGHT\_OPT):

$$f_2(L) = \frac{L}{L_{opt}} e^{\left(1 - \frac{L}{L_{opt}}\right)} \quad (6)$$

Here,  $L$  is the light intensity useful for photosynthesis, calculated as (Jørgensen and Bendoricchio, 2001):

$$L = \alpha \cdot I_0 \cdot e^{-\gamma \cdot h} \quad (7)$$

$k_L$  is called semi-saturation constant,  $\alpha$  is a coefficient accounting for photosynthetic activity,  $I_0$  is the light intensity at the sea surface ( $W m^{-2}$ ),  $\gamma$  is the extinction coefficient in the water body,  $h$  is the depth of the modeled water layer (i.e., 1 m), and  $L_{opt}$  is the optimum light intensity for photosynthesis. The value of  $L_{opt}$  can potentially change according to the acclimation of phytoplankton to light variations over depth and time (Hill, 1963; Jørgensen and Bendoricchio, 2001).

The function  $f_3(N)$  represents the effect of nutrient limitation. The classic Michaelis–Menten kinetics was chosen (Jørgensen and Bendoricchio, 2001):

$$f_3(N) = \frac{N}{k_N + N} \quad (8)$$

where  $\mu_{max}(T_{ref})$  is limited by the external concentration  $N$  of the nutrient (Jørgensen and Bendoricchio, 2001), expressed in micromole  $l^{-1}$ , and  $k_N$  represents the semi-saturation constant, which is inversely related to algal affinity for nutrients. Different ecological models were built to assess the effect on model performance of choosing to simulate only one predetermined limiting nutrient or, rather, the presence of two or three potential limiting nutrients. When more than one potential limiting nutrient was present,  $f_3$  was calculated using Liebig's law of the minimum (henceforth LIEB). For example, in the case of three potential limiting nutrients  $N_1$ ,  $N_2$  and  $N_3$ , such law can be translated as (Jørgensen and Bendoricchio, 2001):

$$f_3(N_1, N_2, N_3) = \min \left( \frac{N_1}{k_{N_1} + N_1}, \frac{N_2}{k_{N_2} + N_2}, \frac{N_3}{k_{N_3} + N_3} \right) \quad (9)$$

Furthermore, some ecological models were tested which contained two different  $k_N$  values for the periods preceding and following the fish-farm closure; this was done to understand if the abrupt cessation of the fish-farm activity produced a radical change in the phytoplankton community composition (and, consequently, in  $k_N$ ). We, thus, assumed that different semi-saturation constants would correspond to different species composition in the community. The loss term  $G$  of Eq. (1) depends on water temperature through an Arrhenius relationship (Jørgensen and Bendoricchio, 2001):

$$G(T) = G(T_{ref}) \cdot \theta_G^{(T - T_{ref})} \quad (10)$$

Similarly to Eq. (3),  $\theta_G$  approximately ranges between 1 and 1.05. As discussed above,  $G$  represents the aggregated effect of several

processes, including grazing. More complex models for grazing than the first order kinetics used in Eq. (1) are commonly used in the literature, e.g. in the so-called NPZ models (Franks, 2002) which explicitly simulate zooplankton population dynamics. However, such models could not be constructed due to a lack of data regarding zooplankton abundance in the Gulf of Aqaba. Our description of grazing (Eq. (1)) represents a simplification of common zooplankton grazing models (Franks, 2002; Jørgensen and Bendoricchio, 2001) obtained by assuming constant grazer biomass (a forced assumption here, given the lack of data). In general, we stress that the separate quantification of grazing and of the other processes summarized by  $G$  would have added unnecessary complexity to the model, leading to model overfitting given the relatively few observations available (Fig. 2), and would have required hitherto unavailable data.

The Simulink tool of MATLAB software was used to build the ecological models. The model construction followed the procedure shown by Jørgensen and Bendoricchio (2001). First, the values of parameters and forcing functions were varied, one by one, to see if the model reacted as expected (model verification). Starting values and plausible ranges for the model parameters were obtained from the ecological literature (Jørgensen et al., 1991) and, when possible, referred to ecosystems similar to the Gulf of Aqaba. These approximate starting values were finally calibrated to obtain a best fit of the model to the observed chlorophyll  $a$  samples. Initially, a manual calibration was performed, and then followed by an automatic calibration using Simulink, which optimized the fitting by minimizing the least-square error given by the difference between empirical observations and model outputs.

Different models were fitted to data and their fitting performance was compared by using two indices, i.e., the Nash–Sutcliffe model efficiency coefficient (Nash and Sutcliffe, 1970; Moriasi et al., 2007):

$$E = 1 - \frac{\sum_{t=1}^T (Q_m^t - Q_o^t)^2}{\sum_{t=1}^T (Q_o^t - \bar{Q}_o)^2} \quad (11)$$

and the Akaike information criterion (AIC) (Burnham and Anderson, 2002):

$$AIC = M \cdot \ln \left( \frac{\sum (Q_m^t - \bar{Q}_o)^2}{M} \right) + 2k \quad (12)$$

where  $Q_m^t$  is the value of the modeled data (chlorophyll  $a$  concentration) at time  $t$ ,  $Q_o^t$  is the observed value of chlorophyll  $a$  at time  $t$ ,  $\bar{Q}_o$  is the average of all the observed data,  $M$  is the number of samples over time, and  $k$  is the number of model parameters (Nash and Sutcliffe, 1970; Akaike, 1974; Burnham and Anderson, 2002; Moriasi et al., 2007). The best models were selected based on the values of these two goodness-of-fit indicators, which provide partially different information. The Nash–Sutcliffe model efficiency ( $E$ ) coefficient assesses the goodness of fit and predictive power of a model. This index can range from  $-\infty$  to 1. If  $E = 1$ , there is a perfect match between the modeled and observed data, while if  $E = 0$ , the model predictions are as accurate as the mean of the observed data. Thus, if  $E < 0$ , the model is useless since it performs worse than the simplest possible model, represented by a horizontal line with an intercept equal to the mean value of the observed data. The closer  $E$  is to 1, the more accurate the model is (Nash and Sutcliffe, 1970; Moriasi et al., 2007). The Akaike information criterion (AIC) also measures the goodness of fit, but it includes a penalty term that is an increasing function of the number of estimated parameters (the second term on the right-hand side of Eq. (12)). This fact is particularly important because  $E$  does not take into account the number of parameters (Nash and Sutcliffe, 1970) and, thus, more complex models would always be favored in the confrontation based on  $E$ .

Instead, AIC highlights the models displaying a balanced compromise between the achievement of a good fit level and the need to avoid the addition of unnecessary complexity to the simulation, i.e., those parsimonious models that do not “overfit” the data. The more negative the AIC index value is, the better the model is.

### 3. Results

#### 3.1. Statistical analyses of time series

NO<sub>3</sub> concentration (Fig. 2A and Table 2) showed a statistically significant difference in the FFS between the two periods, markedly decreasing after the fish-farm closure. The same was true in the STA, but the decrease in nitrate concentration after the end of maricultural activities was weaker than in the FFS. No statistically significant differences in NO<sub>3</sub> concentration either before or after the fish farm closure could be detected between the two sampling stations.

Phosphorus displayed a similar trend to that of nitrogen in the case of the FFS, where a statistically significant decrease in PO<sub>4</sub> concentration after fish-farm closure could be observed. In contrast, in the case of STA, the periods before and after the closure were characterized by similar phosphorus levels (Fig. 2B and Table 2). A comparison of the two sampling stations highlighted a statistically significant difference in PO<sub>4</sub> concentration in the period before the fish-farm closure (Table 2), when the median concentration was higher in the FFS than in STA, but not afterwards.

The pattern of the sampled SiOH<sub>4</sub> concentration over time is presented in Fig. 2C. In the FFS, there were initially strong, short-term fluctuations that ceased approximately three months after the closure of the fish farms. Despite this abrupt change in oscillations, no statistically significant difference in SiOH<sub>4</sub> levels could be detected when comparing the periods preceding and following the end of maricultural activities (Table 2). In the STA, such marked fluctuations were not present, and, similar to the FFS, no statistically significant change in SiOH<sub>4</sub> concentration was detected after the closure of the fish farms. According to the

Wilcoxon matched-pairs test, SiOH<sub>4</sub> concentration tended to be higher in the FFS both in the period before and in the period following the fish-farm closure; however, the difference in median concentration in the latter period became much smaller (Table 2).

Chlorophyll *a* concentration showed a statistically significant and marked decrease in the FFS following the cessation of fish-farm activities, while in the case of the control station, STA, no statistically significant difference could be detected between the chlorophyll *a* levels before and after the end of maricultural activities. Indeed, before the fish-farm closure, chlorophyll *a* concentration was higher in the FFS compared to the STA, but after the closure, such differences between the two stations were much reduced and only weakly significant (Fig. 2D and Table 2).

#### 3.2. Ecological models of phytoplankton dynamics

Several simulations of phytoplankton-population dynamics over time were performed and fitted to the time series of chlorophyll *a* observations in order to test different model structures, characterized by different forcing functions (e.g., different types of nutrients) and combinations of submodels (Table 1). The same types of models were tested for both the FFS and the STA; results are reported in Tables 3 and 4, respectively. In the case of the FFS, several models (7 out of 15) were characterized by  $E > 0$  and, therefore, represented a potentially meaningful description of phytoplankton dynamics. The two indicators used to classify the models according to their performance, namely the Nash-Sutcliffe efficiency criterion ( $E$ , accounting only for the goodness-of-fit), and AIC (an indicator also taking the simplicity of the model into account), ranked the models in exactly the same way (Table 3). The three best models for the FFS (Models 13, 14, and 15) had many traits in common: all of them simulated the effect of temperature through the exponential function (Eq. (3)), the effect of light through a saturation-like function (Eq. (5)), and included nitrates as the nutrient form driving phytoplankton dynamics before the closure of the fish farms. Furthermore, all these models were characterized by a change in the nutrient submodel after the fish-farm

**Table 2**  
Results of the statistical comparison of median concentrations across sampling stations and periods: the first and second columns report the  $U$  statistic from the Mann–Whitney  $U$  test and associated  $p$ -values  $P$  (uncorrected for multiple testing) and  $P_{\text{Adj}}$  (adjusted for multiple testing), while the third and fourth columns report the  $Z$  statistic from the Wilcoxon matched-pairs test and associated  $p$ -values. Median concentrations during the study period for the analyzed station are also reported, expressed as  $\mu\text{mol l}^{-1}$  for nutrients and as  $\mu\text{g l}^{-1}$  for chlorophyll *a*. BFC, before fish-farm closure; AFC, after fish-farm closure; FFS, fish-farm station; STA, Station A. Statistically significant results at significance level  $\alpha = 0.05$  (without correcting for multiple testing) are highlighted: N.S. indicates  $P > 0.05$ ; \* indicates  $P < 0.05$ ; \*\*  $P < 0.01$ ; and \*\*\*  $P < 0.001$ . The symbol # denotes tests in which the null hypothesis is still rejected even after carrying out the Benjamini–Hochberg procedure to correct for multiple testing, with chosen false discovery rate FDR = 0.05 (Benjamini and Hochberg, 1995; Verhoeven et al., 2005).

	Fish-farm station: BFC vs AFC	Station A: BFC vs AFC	BFC: Fish-farm station vs Station A	AFC: Fish-farm station vs Station A
NO <sub>3</sub>	$U = 53.0$ $P = ***$ $P_{\text{Adj}} = 0.003^{\#}$ BFC = 0.43 AFC = 0.03	$U = 89.0$ $P = *$ $P_{\text{Adj}} = 0.063$ BFC = 0.093 AFC = 0.018	$Z = 0.78$ $P = \text{N.S.}$ $P_{\text{Adj}} = 0.47$ FFS = 0.43 STA = 0.09	$Z = 1.92$ $P = \text{N.S.}$ $P_{\text{Adj}} = 0.083$ FFS = 0.030 STA = 0.018
PO <sub>4</sub>	$U = 84.5$ $P = *$ $P_{\text{Adj}} = 0.051$ BFC = 0.057 AFC = 0.031	$U = 142.5$ $P = \text{N.S.}$ $P_{\text{Adj}} = 0.73$ BFC = 0.021 AFC = 0.033	$Z = 2.67$ $P = **$ $P_{\text{Adj}} = 0.024^{\#}$ FFS = 0.057 STA = 0.021	$Z = 0.88$ $P = \text{N.S.}$ $P_{\text{Adj}} = 0.47$ FFS = 0.031 STA = 0.033
Si(OH) <sub>4</sub>	$U = 129.5$ $P = \text{N.S.}$ $P_{\text{Adj}} = 0.47$ BFC = 0.87 AFC = 0.86	$U = 95.0$ $P = \text{N.S.}$ $P_{\text{Adj}} = 0.083$ BFC = 0.59 AFC = 0.79	$Z = 2.96$ $P = **$ $P_{\text{Adj}} = 0.012^{\#}$ FFS = 0.87 STA = 0.59	$Z = 2.30$ $P = *$ $P_{\text{Adj}} = 0.051$ FFS = 0.86 STA = 0.79
Chl- <i>a</i>	$U = 47.5$ $P = ***$ $P_{\text{Adj}} = 0.002^{\#}$ BFC = 0.42 AFC = 0.24	$U = 121.0$ $P = \text{N.S.}$ $P_{\text{Adj}} = 0.40$ BFC = 0.24 AFC = 0.19	$Z = 3.62$ $P = ***$ $P_{\text{Adj}} = 0.002^{\#}$ FFS = 0.42 STA = 0.24	$Z = 2.11$ $P = *$ $P_{\text{Adj}} = 0.063$ FFS = 0.24 STA = 0.19

**Table 3**

Simulation results for the fish-farm station: the table reports the number of the model, the model structure (in terms of the combinations of the submodels from Table 1), the number of the parameters in the model, as well as the efficiency and AIC values. All simulations in this table were based on the FFS data. Simulations are listed in decreasing AIC order, thus, at the top of the table there are the worst simulations and at the bottom the best ones according to such criteria.

Model N°	Model structure (combination of submodels according to Table 1)	Parameters N°	E	AIC
1	T_EXP, SEASON, LIGHT_SAT, KVAR	11	−1.984	−56.344
2	T_EXP, SEASON, LIGHT_SAT	9	−2.107	−58.924
3	T_EXP, LIGHT_OPT	7	−2.225	−61.624
4	T_EXP, NO <sub>3</sub> , LIGHT_OPT, KVAR	9	−1.842	−62.046
5	T_OPT, NO <sub>3</sub>	9	−0.703	−79.981
6	T_OPT, PO <sub>4</sub>	9	−0.429	−86.117
7	T_EXP, PO <sub>4</sub> , NO <sub>3</sub> , SiOH <sub>4</sub> , LIEB	9	−0.406	−86.672
8	T_EXP, LIGHT_SAT	7	−0.046	−101.036
9	T_EXP, PO <sub>4</sub> , KVAR	8	0.139	−105.836
10	T_EXP, PO <sub>4</sub>	7	0.133	−107.614
11	T_EXP, NO <sub>3</sub>	7	0.181	−109.614
12	T_EXP, NO <sub>3</sub> , KVAR	8	0.294	−112.776
13	T_EXP, NO <sub>3</sub> , CHN, SiOH <sub>4</sub> , LIGHT_SAT	9	0.420	−117.698
14	T_EXP, NO <sub>3</sub> , LIGHT_SAT, KVAR	9	0.435	−118.62
15	T_EXP, NO <sub>3</sub> , CHN, PO <sub>4</sub> , LIGHT_SAT	9	0.446	−119.29

**Table 4**

Simulation results for Station A: the table reports the number of the model, the model structure (in terms of the combinations of the submodels from Table 1), the number of parameters in the model, as well as E and AIC values. All simulations in this table were based on STA data. Simulations are listed in decreasing AIC order, thus, at the top of the table there are the worst simulations and at the bottom – the best ones according to such criteria.

Model N°	Model structure (combination of submodels according to Table 1)	Parameters N°	E	AIC
4	T_EXP, NO <sub>3</sub> , LIGHT_OPT, KVAR	9	−1.964	−74.734
15	T_EXP, NO <sub>3</sub> , CHN, PO <sub>4</sub> , LIGHT_SAT	9	−1.827	−76.397
13	T_EXP, NO <sub>3</sub> , CHN, SiOH <sub>4</sub> , LIGHT_SAT	9	−1.730	−77.610
3	T_EXP, LIGHT_OPT	7	−2.035	−77.898
14	T_EXP, NO <sub>3</sub> , LIGHT_SAT, KVAR	9	−1.586	−79.511
6	T_OPT, PO <sub>4</sub>	9	−1.493	−80.798
5	T_OPT, NO <sub>3</sub>	9	−1.177	−85.535
9	T_EXP, PO <sub>4</sub> , KVAR	8	−0.956	−91.290
10	T_EXP, PO <sub>4</sub>	7	−1.053	−91.575
7	T_EXP, PO <sub>4</sub> , NO <sub>3</sub> , SiOH <sub>4</sub> , LIEB	9	−0.692	−94.351
8	T_EXP, LIGHT_SAT	7	−0.857	−95.098
9	T_EXP, NO <sub>3</sub> , KVAR	8	−0.396	−103.099
11	T_EXP, NO <sub>3</sub>	7	−0.412	−104.682
2	T_EXP, SEASON, LIGHT_SAT	9	0.043	−114.314
1	T_EXP, SEASON, LIGHT_SAT, KVAR	11	0.606	−141.390

closure: in the case of Models 13 and 15, the limiting nutrient changed from nitrates to silicates and phosphates, respectively, while in the case of Model 14, the value of the semi-saturation constant for nitrate was changed. These three models displayed very similar *E*'s, which ranged from 0.42–0.45, as well as similar AIC indexes, which were found in a narrow range of values, i.e., within less than 2 units from the best model. Indeed, a value of 2 is the weight given to a parameter in the calculation of AIC (Eq. (12)), and, thus, as a rule of thumb, such a difference in AIC values could be regarded as negligible, given that the three best models displayed the same level of complexity (that is, the same number of parameters) (Burnham and Anderson, 2002). A visual inspection of the plots of the simulation outputs (Fig. 3), however, highlighted some important differences between them: although all the models reasonably reproduced the main trend in chlorophyll *a* concentration as well as the large peak in the spring of 2008, very low or zero values for phytoplankton biomass were found near the end of the simulation period, mainly due to the very low values detected for nutrient concentration, in the case of Models 14 and 15 (Fig. 3).

In the case of the STA (Table 4), only two models displayed positive *E*'s, one being characterized by an efficiency slightly > 0 (Model 2) and another by quite a large efficiency (61%) (Model 1). The latter model was clearly the best one since it also displayed the largest AIC by far, despite the large complexity (11 parameters), and it did not show unrealistic behaviors as in the case of the former model, which predicted zero concentration over the final months of the simulation (Fig. 4). Indeed, a visual inspection showed that

Model 1 was able to quite satisfactorily reproduce the main changes in chlorophyll *a* concentration over time. This result was achieved through a (relatively simple) nutrient submodel representing the seasonality of phytoplankton dynamics in the gulf as well as the effect of the termination of maricultural activities. This submodel simulated that chlorophyll *a* dynamics was limited by NO<sub>3</sub> in winter and spring each year since nitrogen is the nutrient regulating the dynamics of *Cryptophyta* and *Chlorophyta*, which are more abundant in those seasons, whereas PO<sub>4</sub> was the limiting nutrient form in summer and fall since phosphorus regulates the abundance of *Prochlorococcus* and *Synechococcus*, which dominate the producer community during that period (Al-Najjar et al., 2007; Mackey et al., 2007; Mackey et al., 2009). Such seasonal changes in the limiting nutrient were present in both Models 1 and 2 (Table 4). Model 1, however, displayed additional complexity since the semi-saturation constant for the simulated nutrients ( $k_N$  in Eq. (8)) was allowed to change its value after the closure of the fish farms, to simulate a relatively abrupt change in the phytoplankton composition following the reduction of nutrient inputs from coastal activities. This simple application of a structurally dynamic submodel (Jørgensen and Bendricchio, 2001) to describe the effect of mariculture, greatly improved the goodness-of-fit of the simulation with respect to the simpler Model 2, in particular after the fish-farm closure (Fig. 4).

A comparison of Tables 3 and 4 shows that the best models for the FFS (Models 13, 14, and 15) are those with the worst performance in the case of the STA, and vice versa (Models 1 and

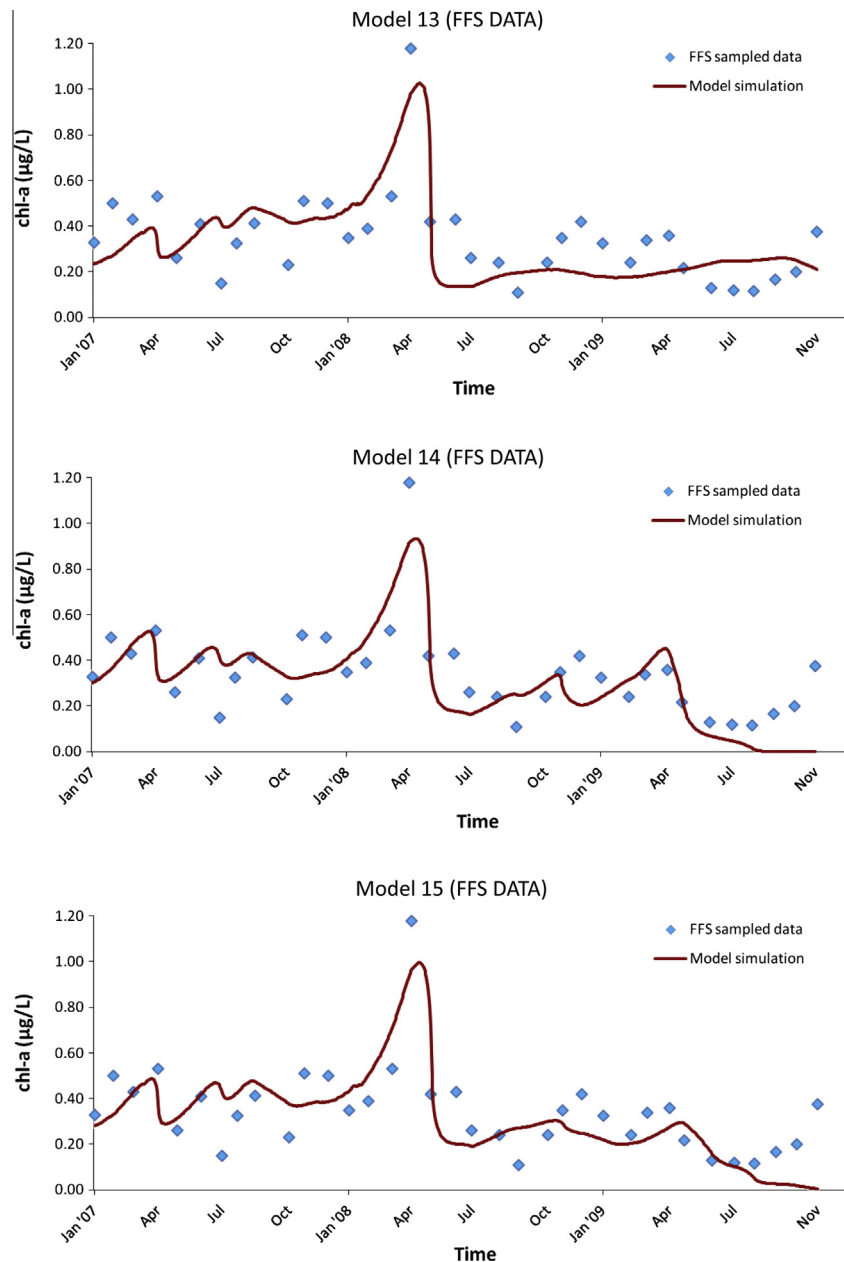


**Fig. 3.** The fit of the best models of phytoplankton dynamics for the fish-farm station dataset: the continuous lines represent Model 13, 14, and 15 (Table 3), respectively, while diamonds represent observations. All three models are approximately equivalent in terms of AIC, but phytoplankton becomes extinct at the end of the simulation in the case of Model 14.

2 are the worst ones in the the FFS and the best ones in the STA), suggesting that micro-algal dynamics at the two sites is, at least partially, driven by different processes. However, the best models at the two sites also share some traits: remarkably, for both sampling stations, all the best models simulated the effect of temperature on phytoplankton growth through the exponential function (Eq. (3)) and that of light through a saturation-like function (Eq. (5)). Indeed, the models containing such monotonic submodels of light and temperature outperformed their counterpart models, which only differed from them because they contained humped, optimum submodels describing the dependence on those forcing functions (Model 3 versus Model 8, Model 4 versus Model 14, Model 5 versus Model 11, and Model 6 versus Model 10; Tables 3 and 4). The fitted parameters for the best models of the FFS and STA are reported in Table 5.

## 4. Discussion

### 4.1. Statistical analysis of time series

The end of maricultural activities in the Gulf of Aqaba coincided with a decrease in the concentration observed for phosphorus and nitrogen, as well as with the disappearance of the oscillations in silicate concentration, in the sampling site near the coast (FFS). In particular, nitrates showed a remarkable reduction since the ratio of the median concentration before the closure of the fish farm to the median after the closure was about 14. These changes corresponded to a reduction in chlorophyll *a* concentration at the FFS, which could, therefore, be explained as a consequence of the reduced nutrient availability. Indeed, our analysis of the nutrient and chlorophyll *a* time series strongly suggests that the fish-farm



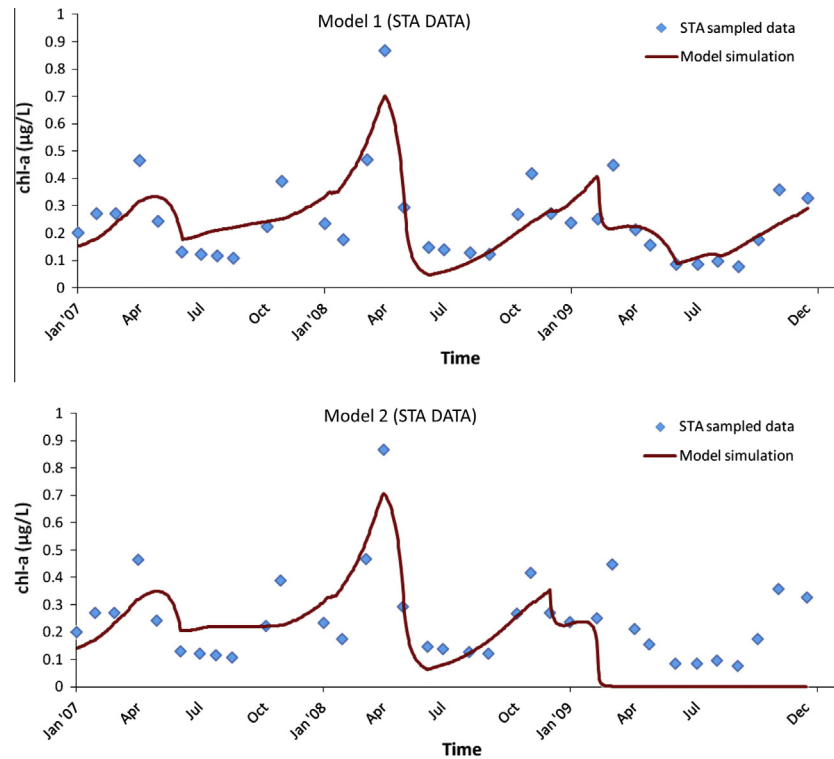


**Fig. 4.** The fit of the best models of phytoplankton dynamics for the Station A dataset: the continuous lines represent Models 1 and 2 (Table 4), respectively, while diamonds represent observations. Only Model 1, representing the best simulation for this sampling site, has a clearly positive performance in describing chlorophyll *a* observations, while in the case of Model 2 phytoplankton becomes extinct during the third year of simulation.

**Table 5**

Fitted model parameters and initial conditions for the “best” model for the FFS (Models 13–15) and STA (Model 1): BFC, before fish-farm closure; AFC, after fish-farm closure; FFS, fish-farm station; STA, Station A. Chlorophyll *a* at time = 0 is the initial value of the chlorophyll *a* concentration at the simulation start;  $\mu_{max}$  is the phytoplankton maximum growth rate (Eq. (2));  $G$  is the single loss parameter (grazing, respiration, exudation, non-predatory mortality and settling) (Eq. (1));  $\theta$  is the parameter for the Arrhenius exponential model referring to the phytoplankton maximum growth rate  $\mu_{max}$ , while  $\theta_G$  similarly refers to the single loss parameter  $G$ ;  $T_{ref}$  (Eq. (2), (3), and (10)) is the reference temperature,  $K_L$  is the semi-saturation constant for the light function (Eq. (5)).  $K_N$  is the semi-saturation constant for  $NO_3$ ,  $K_P$  for  $PO_4$ , and  $K_S$  for  $SiOH_4$  in Eq. (8).

Parameter	Fitted value			
	Model 13 – FFS	Model 14 – FFS	Model 15 – FFS	Model 1 – STA
Chlorophyll <i>a</i> at time = 0	0.235	0.241	0.281	0.152
$\mu_{max}$	0.986	0.993	0.989	0.997
$G$	0.968	0.974	0.970	0.976
$\theta$	1.0309	1.0308	1.0309	1.0307
$\theta_G$	1.0315	1.0314	1.0315	1.0313
$T_{ref}$	24.059	24.059	24.058	24.051
$K_L$	1.123	1.111	1.024	1.214
$K_N$ BFC	0.00227	0.00237	0.00281	
$K_N$ AFC		0.00042		
$K_S$ AFC	0.00808			
$K_P$ AFC			0.000465	
$K_N$ (during winter and spring) BFC				0.00253
$K_P$ (during summer and fall) BFC				0.0000766
$K_N$ (during winter and spring) AFC				0.000284
$K_P$ (during summer and fall) AFC				0.0000377

activities had altered the quality of water near the coast in the northernmost part of the Gulf of Aqaba through the emission of large nutrient fluxes, which were fuelling an abnormally high phytoplankton biomass (Huang et al., 2011; Donald et al., 2013). Observations at the control station (STA), which is farther from the fish farms, did not show any changes in nutrient concentration or chlorophyll *a* following the end of the maricultural activities, with the partial exception of a weak reduction in nitrate concentration, suggesting that the abrupt variations in environmental parameters observed at the FFS were mainly the result of human

activities rather than of natural oscillations (e.g., upwelling or advection of nutrient-rich waters through currents) in the marine ecosystem that, if present, should have been detected at the control station. The slightly significant reduction in nitrate concentration observed at the STA can be explained in at least two manners: it could mean that the effect of the end of maricultural activities on nutrient levels could be detected, albeit weakly, even at such a large distance from the fish farms, or, alternatively, that a reduction in nitrogen concentration due to other causes than the fish-farm closure also took place in the basin during the period

following the fish-farm closure (e.g., as a result of the above-mentioned natural oscillations in the marine ecosystem) and also affected nutrient concentration.

The hypothesis that maricultural activities had perturbed the natural level of nutrients close to the coast is supported by the results of the Wilcoxon matched-pairs test. Indeed, before the closure of the fish farms, the concentration of several nutrients (P, Si) and of chlorophyll *a* was markedly higher in the FFS than in the STA, while after the closure, the concentration of P at the two sampling sites became indistinguishable and the previously observed differences in Si and chlorophyll *a* concentration between the FFS and the STA became weaker. These results suggest that once the human impact had stopped, nutrient concentration and phytoplankton at the coastal site tended to become more similar to those of the unperturbed (or less perturbed) control site in the open ocean. The weak difference in the concentration of silicate and chlorophyll *a* that was still present between the two sampling sites after the fish-farm closure, can be due to fact that the recovery of the FFS ecosystem from fish-farm perturbation was not an instantaneous process but, rather, that the cycling of the excess nutrients of human origin out of the food web took some time. Another possible explanation is that other natural or human sources of nutrients besides those related to the fish-farming activity were present on the mainland and caused higher nutrient concentrations (and, consequently, higher phytoplankton biomass) closer to the coast (Chen et al., 2008; Lazar et al., 2008).

The tight relationship between chlorophyll *a* and nutrient levels emerging from the analysis of the time series is, indeed, an ecological feature to be expected in oligotrophic ecosystems such as the Gulf of Aqaba (Chen et al., 2008; Lazar et al., 2008). This relationship is evident in the case of the peak in  $\text{NO}_3$  and  $\text{PO}_4$  concentration in late winter – early spring of 2008, which resulted in a slightly lagged boost in the chlorophyll *a* time series (Fig. 2). Such a marked increase in nutrient concentration was probably produced by the intense mixing (Iluz et al., 2009) and corresponded to a strong spring bloom in the phytoplankton community (Gordon et al., 1994; Genin et al., 1995), given that N and, in particular, P are the two main limiting nutrients for phytoplankton growth in the Gulf of Aqaba (Suggett et al., 2009). This example demonstrates that natural variability in the ecosystem, in addition to anthropogenic nutrient enrichment, can strongly influence the coupled nutrient-algal dynamics in the gulf. The processes of natural and human enrichment of the ecosystem are, however, quite different, since the former is characterized by isolated boosts in nutrient concentration while the latter causes a permanent increase in nutrient levels, although some variability can still be observed (Fig. 2). For this reason, these two processes can be expected to yield different types of impact on the ecosystem of the Gulf of Aqaba.

#### 4.2. Ecological models of phytoplankton dynamics

The confrontation of different simulation models (combinations of submodels and functions from Table 1) and their ability to reproduce field measurements (Hilborn and Mangel, 1997) is a useful exercise for shedding light on the key processes influencing the dynamics of an ecosystem. Indeed, only a few models provided an acceptable fit (that is, positive Nash–Sutcliffe efficiency) to the observed time series of chlorophyll *a*, and an even smaller number of models clearly outperformed the others according to the AIC criterion. In agreement with the results of the statistical analyses, the best simulations in the case of the FFS highlighted that the most accurate way to describe the population dynamics of phytoplankton was to include an abrupt, discontinuous change in the nutrient submodel, be it in the limiting nutrient – shifting from nitrogen to silicon or phosphorus (Models 13 and 15), or in the composition of the algal community (as represented by the changing value of the

semi-saturation constant in Model 14, which is a simple example of a structurally dynamic model; see Jørgensen and Bendoricchio, 2001). Such a common feature of the best models indirectly supports the hypothesis that maricultural activities had affected nutrient concentrations in the FFS since such an abrupt change was chosen to be coincident with the closure of the fish farms.

Importantly, the choice of using process-based models allowed us to link these abrupt changes in nutrient levels to the observed decrease in the chlorophyll *a* concentration in a quantitative and ecologically sound manner, i.e., we could demonstrate that the observed phytoplankton dynamics were quantitatively consistent with ecological processes, such as nutrient enrichment and limitation, which take place in the ocean. Indeed our process-based modeling approach overcomes the several well-known limitation of simple indicators used in eutrophication management such as the Redfield ratio (Jørgensen and Bendoricchio, 2001; furthermore, representative time series of ecologically-relevant Si:N:P ratios could not be calculated as  $\text{NO}_2$  and  $\text{NH}_4^+$  measurements contained too many gaps). In the Gulf of Aqaba, the observed, typical seasonal dynamics shows that when the nutrient concentrations are very low, in particular in summer and fall, *Prochlorococcus* and *Synechococcus* represent a significant portion of the phytoplankton community; these taxa are characterized by higher phosphorous requirements compared to nitrogen (Agawin et al., 2007; Al-Najjar et al., 2007; Mackey et al., 2007; Mackey et al., 2009). During winter and spring, when there is a strong mixing, nutrients are brought from the deep water layers. In that period of the year, *Cryptophyta* and *Chlorophyta* account for most of the phytoplankton community that is generally limited by light, but not in the upper euphotic zone analyzed here, where, in this case, nitrogen best explains the chlorophyll *a* dynamics (Mackey et al., 2009). Therefore, an increase in nutrient concentrations, be it caused by mixing or by fish-farm activities, is expected to cause a change in phytoplankton dynamics and an increase in phytoplankton biomass (Flander-Puttle and Malej, 2003; Takamura et al., 1992), as observed in the models. According to the best models in the FFS, the disappearance of the nutrient inputs emitted from the fish farms is consistent with an abrupt reduction in the phytoplankton-community biomass and/or a marked change in its composition.

Importantly, the choice of driving the models by using sampled nutrient concentrations and measurements of water temperature allowed us to simulate the effect of seasonal mixing, which is well-known to have a key role in the Gulf of Aqaba ecosystem, and of atmospheric deposition, even when using a simple zero-dimensional model (Eq. (1)). Indeed, the concentration of nutrients in the Gulf of Aqaba is strongly influenced by mixing events (Iluz et al., 2009; Al-Najjar et al., 2007; Mackey et al., 2007), therefore the choice of using measured nutrient concentrations as a forcing function indirectly accounts for the influence of seasonal mixing on phytoplankton in the models. The same considerations hold true for the relationship between water temperature and mixing, and for the relationship between nutrient concentration and atmospheric deposition.

A feature shared by the best simulations in the FFS is that nitrogen was always the only nutrient limiting phytoplankton growth in the period before the fish-farm closure, i.e., during fish farm activity, the phytoplankton dynamics was primarily driven by the surface nitrogen concentration. Since this result contradicts the above-mentioned observation that some of the algal taxa typically dominating the Gulf of Aqaba in summer and fall (*Prochlorococcus* and *Synechococcus*) are phosphorus-limited (Fuller et al., 2005; Mackey et al., 2009), it suggests that the impact of fish farming altered the typical phytoplankton dynamics as well as the usual seasonal succession of algal taxa in the area (indeed, Models 1 and 2, which simulate such seasonal succession, performed very poorly in the FFS, Table 3). We can speculate that during all the seasons of

the period of ongoing maricultural activities (including summer and fall), the species that represented the major fraction of the phytoplankton community at the FFS were those typically present in the Gulf of Aqaba only during winter and spring, with a high nutrient concentration (*Cryptophyceae* and *Chlorophyceae*). In contrast, during fish-farm activity, *Prochlorococcus* and *Synechococcus* were probably scarcely present since they tend to dominate the phytoplankton community in terms of biomass during summer and fall, when nutrient concentration is low (Al-Najjar et al., 2007; Mackey et al., 2007; Mackey et al., 2009).

After the closure of the fish farms, different combinations of limiting nutrients gave similar results for the FFS and there is not a single solution which seems most plausible (see Models 13, 14 and 15 in Table 3; however, the choice of phosphorus (Model 15) is consistent with the fact that nutrient scarcity due to fish-farm closure is expected to be associated with taxa, such as *Prochlorococcus* and *Synechococcus*, which are phosphorus-limited (Al-Najjar et al., 2007; Mackey et al., 2007; Mackey et al., 2009). One possible explanation is that after the fish-farm closure, the chlorophyll *a* concentration became more evenly distributed among the different phytoplankton taxa, whose abundances were limited by different nutrients, i.e., community co-limitation (Arrigo, 2005). Thus, in this case, each nutrient would be a good predictor of the abundance of some (but not all) phytoplankton taxa. This explanation appears consistent with the observations that anthropogenic stressors, such as nutrient enrichment, can reduce the diversity of aquatic communities (Odum, 1985; Caddy, 2000) and of phytoplankton, in particular, during blooms (Irigoin et al., 2004).

In the STA, the main processes driving phytoplankton abundance appear to be partly different from those in the FFS, based on a comparison of the best models at the two stations. To obtain a good model fit for the control sampling site, seasonality in algal dynamics had to be simulated (Models 1 and 2) through a seasonal change in the limiting nutrient. In summer and fall,  $\text{PO}_4$  was chosen as the limiting nutrient since it regulates the growth of most of the taxa composing the phytoplankton community in that period of the year (*Prochlorococcus* and *Synechococcus*) (Al-Najjar et al., 2007; Mackey et al., 2007; Mackey et al., 2009). In winter and spring,  $\text{NO}_3$  was selected as the limiting nutrient since it regulates the growth of *Cryptophyta* and *Chlorophyta*, which are more abundant in winter and when nutrient concentrations are higher (Al-Najjar et al., 2007; Mackey et al., 2007; Mackey et al., 2009).

It was not possible to recreate such seasonal succession of phytoplankton taxa directly in the model, i.e., we could not separately simulate the two dominant phytoplankton groups, because this choice would have doubled the number of model parameters, leading to a much-too-complex model with respect to the few chlorophyll *a* measurements available. Even such a simple simulation of the seasonal succession of algal taxa, however, allowed us to achieve a decent fitting of chlorophyll *a* (Model 2, see Fig. 4). Interestingly, the best model in the case of the STA featured a discontinuity in the nutrient limitation submodel (Model 1), similar to the best FFS simulations, suggesting, as already discussed above, that maricultural nutrient inputs could have reached even this station far from the coast, or, alternatively, that a natural shift in the marine ecosystem took place concomitantly with the closure of the fish farms (however, to our knowledge, in the scientific literature there are no reports of natural events in this period that could have caused a shift in the phytoplankton community). Thus, the modeling results suggest that in the STA, the typical seasonal succession in the Gulf of Aqaba of *Cryptophyta* and *Chlorophyta* (Al-Najjar et al., 2007) associated with nitrogen, and *Prochlorococcus*, and *Synechococcus* (Lindell and Post, 1995; Post et al., 1996) limited by phosphorus, never ceased during the study period and, thus, presumably, the control site was not as perturbed as the FFS

(where the best models did not include any seasonal pattern), although a sudden change in the algal community also took place in the STA after the fish farms had closed. This sudden change, represented in the model as the variation of the values of the two semi-saturation constants (one constant for winter-spring and one for summer-fall), was probably not as marked as in the FFS since the above-mentioned seasonal alternation of taxa did not disappear. Such change in the semi-saturation constant for a given season could, for example, reflect the increased dominance of the phytoplankton community by some species that were already typically present (but not previously so abundant) during that season.

The finding that a weaker change took place in the STA as compared to the FFS is consistent with the results of the statistical analyses, which detected less and weaker (in the case of  $\text{NO}_3$ ) changes in the control station as compared to the FFS when comparing the periods preceding and following the fish-farm closure. Thus, summing up, the best model for the STA suggests that the main process controlling phytoplankton dynamics in that sampling station is the mixing of the water column and, as a consequence, the changes in nutrient concentration, which determine the seasonal succession in the algal community; but, at the same time, this model suggests that the fish-farm activity could have affected micro-algae in that area of the Gulf of Aqaba, albeit more weakly than in the case of the FFS.

An interesting feature shared by all the best models for the FFS and STA is that the best way of describing the dependence of algal growth on temperature and light was through monotonically increasing functions, i.e., the exponential and the Michaelis-Menten relationships, respectively. Indeed, optimum-like relationships between growth and temperature (or light) appear reasonable when studying single populations but, in this study, the models were fitted to changes in chlorophyll *a* concentration over time, which instead reflects the changes in the abundance of the whole phytoplankton community, potentially comprising numerous species. Different phytoplankton species are characterized by different optimum temperatures for growth and, therefore, the exponential function appears as a proper description of the aggregate response of the phytoplankton community to warming waters, where cold-water species are replaced by more thermophilic species since such a function can be considered as the sum of several optimum-like functions (Bowie et al., 1985). A similar explanation can be advocated to justify why a saturation-like relationship of algal growth with light availability seems to be a better submodel than a humped relationship: the numerous species composing phytoplankton can be characterized by different optimal levels of light and, thus, a single optimum for the whole algal community cannot possibly exist.

## 5. Conclusions

Phytoplankton dynamics represents a useful indicator of water quality that can be used to monitor coastal pollution (Boyer et al., 2009). The statistical analyses and the model confrontation in this work show that fish-farming activities in the Gulf of Aqaba strongly altered local nutrient concentrations and, consequently, the dynamics of phytoplankton, which – under the usual conditions of the northern Gulf – should have been dominated by the annual mixing event (Wolf-Vecht et al., 1992; Labiosa et al., 2003; Al-Najjar et al., 2007). A positive correlation between maricultural activities and chlorophyll *a* concentration was clearly apparent from a visual inspection of the sampling time series, as well as by statistical tests, strongly suggesting that anthropogenic nutrient inputs to the basin can markedly alter the abundance and composition of the community of micro-algae, consistently with the oligotrophic, nutrient-limited status of the Gulf of Aqaba ecosystem. The application of deterministic models allowed us to

simulate the ecological processes affecting primary producers and to test in a *quantitative* manner the relative influence of such processes on phytoplankton dynamics. In particular, the simulations showed that, during the activity of the fish farms, nitrogen limitation was the main process influencing phytoplankton dynamics in the FFS and, thus, that the impact of fish farms upon phytoplankton was mediated by their contribution to the changes in the availability of this nutrient. The closure of the fish farms was clearly mirrored by a change in the phytoplankton dynamics, which can be interpreted as a return towards a state unperturbed by farming activities. After the fish farm closure, equally good fits of chlorophyll *a* observations in the FFS could be obtained using different combinations of limiting nutrients, suggesting the establishment of community co-limitation (Arrigo, 2005) and, thus, possibly reflecting an increase in the diversity of the algal community with respect to the situation before the fish farm closure when phytoplankton biomass dynamics in the FFS appeared to be chiefly driven by nitrogen (suggesting that the algal community was dominated only by few taxa such as *Chlorophyceae* and *Cryptophyceae*). Our hypothesis of increased phytoplankton diversity following the reduction in nutrient inputs from fish farming cannot be tested since no data on cell counts are available, however it is consistent with the commonly held interpretation of eutrophication, which is expected to reduce community diversity and favor few fast-responding *r*-strategist, opportunistic species (Cottingham and Carpenter, 1998; Pitta et al., 1998). Our study shows that the Gulf of Aqaba is an exemplary case of a marine ecosystem where physical processes (mixing) drive chemistry (nutrient availability) and finally lead to a biological response (phytoplankton growth), and of how this sequence can be perturbed by human impacts. Proof of the high intensity of the impact of mariculture in the FFS includes the marked changes in nutrient and chlorophyll *a* concentration following the closure of fish farming, but also the fact that all the best simulations for that station do not include seasonality. This suggests that the usual seasonal succession of algal taxa in the ecosystem was clearly perturbed or overshadowed by the effects of anthropogenic nutrient enrichment. In contrast, in the STA, phytoplankton seasonality had to be modeled to obtain good simulation, suggesting a less perturbed site, although the structure of the best model is also consistent with a fish-farming impact, albeit a weaker one compared to the FFS. In conclusion, our work demonstrates that it is useful to apply ecological models together with classical statistical analyses. Process-based models can provide a large amount of information regarding the changes that take place in ecosystems and what causes them; in particular, causes cannot be deduced based on statistical correlation approaches, while models can be used to advance hypotheses about ecosystem functioning and test them in a mechanistic and quantitative fashion, based on our best knowledge regarding ecological processes taking place in the sea. For example, the features of all the best models identified in this study and their quantitative agreement with observations made us hypothesize that an abrupt change in the species composition of the phytoplankton community took place in the Gulf of Aqaba following the end of fish-farm activities; such an abrupt change in the algal community composition could not have been even speculated about based on the simple inspection or classical correlation analysis of the chlorophyll *a* time series presented in this paper.

## Acknowledgments

This study was supported by the programme “The NATO Science for Peace and Security Program (SPS)”, SFP-981883: Protecting the Gulf of Aqaba from Anthropogenic and Natural Stress. Leonardo Laiolo acknowledges support from the faculty of “Mathematical, Physical and Natural Sciences”, Alma Mater Studiorum, Bologna

University, through a thesis abroad scholarship award which allowed him to take part in this project in Israel (Mina & Everard Goodman Faculty of Life Sciences, Bar-Ilan University, Ramat-Gan and Interuniversity Institute for Marine Sciences, Eilat). Alberto Barausse acknowledges support from the European Community's Seventh Framework Programme under grant agreement no. 226675, KnowSeas project. We thank Ms. Sharon Victor of Bar-Ilan University for the English editing.

## References

- Agawin, N.S.R., Rabouille, S., Veldhuis, M.J.W., Servatius, L., Hol, S., Van Overzee, H.M.J., Huisman, J., 2007. Competition and facilitation between unicellular nitrogen-fixing cyanobacteria and non-nitrogen-fixing phytoplankton species. *Limnol. Oceanogr.* 52, 2233–2248.
- Akaike, H., 1974. New look at statistical-model identification. *IEEE T Automat. Contr.* 19, 716–723.
- Al-Najjar, T., Badran, M.I., Richter, C., Meyerhoefer, M., Sommer, U., 2007. Seasonal dynamics of phytoplankton in the Gulf of Aqaba, Red Sea. *Hydrobiologia* 579, 69–83.
- Al-Qutob, M., Häse, C., Tilzer, M.M., Lazar, B., 2002. Phytoplankton drives nitrite dynamics in the Gulf of Aqaba, Red Sea. *Mar. Ecol. Prog. Ser.* 239, 233–239.
- Arrigo, K.R., 2005. Marine microorganisms and global nutrient cycles. *Nature* 437, 349–355.
- Aure, J., Stigebrandt, A., 1990. Quantitative estimates of the eutrophication effects of fish farming on fjords. *Aquaculture* 90, 135–156.
- Benjamini, Y., Hochberg, Y., 1995. Controlling the false discovery rate – a practical and powerful approach to multiple testing. *J. Royal Stat. Soc. B-Met.* 57, 289–300.
- Bowie, G.L., Mills, W.B., Porcella, D.B., Campbell, C.L., Pagenkopf, J.R., Rupp, G.L., Johnson, K.M., Chan, P.W.H., Gherini, S.A., 1985. Rates, constants, and kinetics formulations in surface water quality modeling, second ed. U.S. Environmental Protection Agency, Athens, GA.
- Boyer, J.N., Kelble, C.R., Ortner, P.B., Rudnick, D.T., 2009. Phytoplankton bloom status: Chlorophyll *a* biomass as an indicator of water quality condition in the southern estuaries of Florida, USA. *Ecol. Indic.* 9, S56–S67.
- Brown, J.R., Gowen, R.J., McLusky, D.S., 1987. The effect of salmon farming on the benthos of a Scottish sea loch. *J. Exp. Mar. Biol. Ecol.* 109, 39–51.
- Burnham, K.P., Anderson, D.R., 2002. Model selection and multimodel inference. A practical information-theoretic approach, second ed. Springer Science and Business Media Inc., New York.
- Caddy, J.F., 2000. Marine catchment basin effects versus impacts of fisheries on semi-enclosed seas. *ICES J. Mar. Sci.* 57, 628–640.
- Chen, Y., Mills, S., Street, J., Golan, D., Post, A., Jacobson, M., Paytan, A., 2007. Estimates of atmospheric dry deposition and associated input of nutrients to Gulf of Aqaba seawater. *J. Geophys. Res.-Atmos.* 112: Art. D04309; DOI 10.1029/2006jd007858.
- Chen, Y., Paytan, A., Chase, Z., Measures, C., Beck, A.J., Sanudo-Wilhelmy, S.A., Post, A.F., 2008. Sources and fluxes of atmospheric trace elements to the Gulf of Aqaba, Red Sea. *J. Geophys. Res.-Atmos.* 113: Art. D05306; DOI 10.1029/2007jd009110.
- Cottingham, K.L., Carpenter, S.R., 1998. Population, community, and ecosystem variates as ecological indicators: phytoplankton responses to whole-lake enrichment. *Ecol. Appl.* 8, 508–530.
- Donald, D.B., Bogard, M.J., Finlay, K., Bunting, L., Leavitt, P.R., 2013. Phytoplankton-specific response to enrichment of phosphorus-rich surface waters with ammonium, nitrate, and urea. *PLOS One* 8.
- Flander-Putrlé, V., Malej, A., 2003. The trophic state of coastal waters under the influence of anthropogenic sources of nutrients (fish farm, sewage outfalls). *Period. Biol.* 105, 359–365.
- Franks, P.J.S., 2002. NPZ models of plankton dynamics: their construction, coupling to physics, and application. *J. Oceanogr.* 58, 379–387.
- Fuller, N.J., West, N.J., Marie, D., Yallop, M., Rivlin, T., Post, A.F., Scanlan, D.J., 2005. Dynamics of community structure and phosphate status of picocyanobacterial populations in the Gulf of Aqaba, Red Sea. *Limnol. Oceanogr.* 50, 363–375.
- Genin, A., Lazar, B., Brenner, S., 1995. Vertical mixing and coral death in the Red Sea following the eruption of Mount Pinatubo. *Nature* 377, 507–510.
- Gordon, N., Angel, D.L., Neori, A., Kress, N., Kimor, B., 1994. Heterotrophic dinoflagellates with symbiotic cyanobacteria and nitrogen limitation in the Gulf of Aqaba. *Mar. Ecol. Prog. Ser.* 107, 83–88.
- Grasshoff, K., Kremling, K., Ehrhardt, M., 1999. *Methods of Seawater Analysis*. Wiley-VCH, New York.
- Häse, C., Al-Qutob, M., Dubinsky, Z., Ibrahim, E.A., Lazar, B., Stambler, N., Tilzer, M.M., 2006. A system in balance? Implications of deep vertical mixing for the nitrogen budget in the northern Red Sea, including the Gulf of Aqaba (Eilat). *Biogeosci. Discuss.* 3, 383–408.
- Hilborn, R., Mangel, M., 1997. *The Ecological Detective. Confronting Models with Data*. Princeton University Press, Princeton.
- Hill, M.N., 1963. Global coastal ocean upscale interdisciplinary processes. The composition of sea-water: Comparative and descriptive oceanography. Cambridge, MA, and London: General Editor.
- Huang, Y.C.A., Hsieh, H.J., Huang, S.C., Meng, P.J., Chen, Y.S., Keshavmurthy, S., Nozawa, Y., Chen, C.A., 2011. Nutrient enrichment caused by marine cage



- culture and its influence on subtropical coral communities in turbid waters. *Mar. Ecol. Prog. Ser.* 423, 83–93.
- Iluz, D., Yehoshua, Y., Dubinsky, Z., 2008. Quantum yields of phytoplankton photosynthesis in the Gulf of Aqaba (Eilat), Northern Red Sea. *Israel J. Plant Sci.* 56, 29–36.
- Iluz, D., Dishon, G., Capuzzo, E., Meeder, E., Astoreca, R., Montecino, V., Znchor, P., Ediger, D., Marra, J., 2009. Short-term variability in primary productivity during a wind-driven diatom bloom in the Gulf of Eilat (Aqaba). *Aquat. Microb. Ecol.* 56, 205–215.
- Irigoien, X., Huisman, J., Harris, R.P., 2004. Global biodiversity patterns of marine phytoplankton and zooplankton. *Nature* 429, 863–867.
- Jørgensen, S.E., Bendoricchio, G., 2001. *Fundamentals of Ecological Modelling*, third ed. Elsevier, Amsterdam.
- Jørgensen, S.E., Nielsen, S.N., Jørgensen, L.A., 1991. *Handbook of ecological parameters and ecotoxicology*. Elsevier, Amsterdam.
- Labiosa, R.G., Arrigo, K.R., Genin, A., Monismith, S.G., van Dijken, G., 2003. The interplay between upwelling and deep convective mixing in determining the seasonal phytoplankton dynamics in the Gulf of Aqaba: evidence from SeaWiFS and MODIS. *Limnol. Oceanogr.* 48, 2355–2368.
- Lazar, B., Erez, J., Silverman, J., Rivlin, T., Rivlin, A., Dray, M., Meeder, M., Iluz, D., 2008. Recent environmental changes in the chemical-biological oceanography of the Gulf of Aqaba (Eilat). In: Por, F.D. (Ed.), *Aqaba-Eilat, the improbable gulf. Environment, Biodiversity and Preservation*. Magnes Press, Jerusalem. pp. 49–62.
- Levanon-Spanier, L., Padan, E., Reiss, Z., 1979. Primary production in desert-enclosed sea the Gulf of Elat (Aqaba), Red Sea. *Deep-Sea Res.* 26, 673–685.
- Lindell, D., Post, A.F., 1995. Ultraphytoplankton succession is triggered by deep winter mixing in the Gulf of Aqaba (Eilat), Red Sea. *Limnol. Oceanogr.* 40, 1130–1141.
- Loya, Y., Kramarsky-Winter, E., 2003. In situ eutrophication caused by fish farms in the northern Gulf of Eilat (Aqaba) is beneficial for its coral reefs: a critique. *Mar. Ecol. Prog. Ser.* 261, 299–303.
- Loya, Y., Lubinevsky, H., Rosenfeld, M., Kramarsky-Winter, E., 2004. Nutrient enrichment caused by in situ fish farms at Eilat, Red Sea is detrimental to coral reproduction. *Mar. Pollut. Bull.* 49, 344–353.
- Mackey, K.R.M., Labiosa, R.G., Calhoun, M., Street, J.H., Post, A.F., Paytan, A., 2007. Phosphorus availability, phytoplankton community dynamics, and taxon-specific phosphorus status in the Gulf of Aqaba, Red Sea. *Limnol. Oceanogr.* 52, 873–885.
- Mackey, K.R.M., Rivlin, T., Grossman, A.R., Post, A.F., Paytan, A., 2009. Picophytoplankton responses to changing nutrient and light regimes during a bloom. *Mar. Biol.* 156, 1531–1546.
- Mann, H.B., Whitney, D.R., 1947. On a test of whether one of two random variables is stochastically larger than the other. *Ann. Math. Stat.* 18, 50–60.
- Moberg, F., Folke, C., 1999. Ecological goods and services of coral reef ecosystems. *Ecol. Econ.* 29, 215–233.
- Monismith, S.G., Genin, A., Reidenbach, M.A., Yahel, G., Koseff, J.R., 2006. Thermally driven exchanges between a coral reef and the adjoining ocean. *J. Phys. Oceanogr.* 36, 1332–1347.
- Moriasi, D.N., Arnold, J.G., Van Liew, M.W., Bingner, R.L., Harmel, R.D., Veith, T.L., 2007. Model evaluation guidelines for systematic quantification of accuracy in watershed simulations. *T. Asabe* 50, 885–900.
- Nash, J.E., Sutcliffe, J.V., 1970. River flow forecasting through conceptual models part I – A discussion of principles. *J. Hydrol.* 10, 282–290.
- Odum, E.P., 1985. Trends expected in stressed ecosystems. *Bioscience* 35, 419–422.
- Parsons, T.R., Maita, Y., Lalli, C.M., 1984. *A Manual of Chemical and Biological Methods for Seawater Analysis*. Pergamon Press, Oxford.
- Paytan, A., McLaughlin, K., 2007. The oceanic phosphorus cycle. *Chem. Rev.* 107, 563–576.
- Paytan, A., Mackey, K.R.M., Chen, Y., Lima, I.D., Doney, S.C., Mahowald, N., Labiosa, R., Post, A.F., 2009. Toxicity of atmospheric aerosols on marine phytoplankton. *Proc. Natl. Acad. Sci. USA* 106, 4601–4605.
- Pitta, P., Karakassis, I., Tsapakis, M., Zivanovic, S., 1998. Natural vs. mariculture induced variability in nutrients and plankton in the eastern Mediterranean. *Hydrobiologia* 391, 181–194.
- Post, A.F., Veldhuis, M., Lindell, D., 1996. Spatial and temporal distribution of ultraphytoplankton in the Gulf of Aqaba, Red Sea. *J. Phycol. Suppl.* 32, 38–39.
- Richter, C., Wunsch, M., Rasheed, M., Kotter, I., Badran, M.I., 2001. Endoscopic exploration of Red Sea coral reefs reveals dense populations of cavity-dwelling sponges. *Nature* 413, 726–730.
- Shapiro, S.S., Wilk, M.B., Chen, H.J., 1968. A comparative study of various tests for normality. *J. Am. Stat. Assoc.* 63, 1343–1372.
- Siegel, S., Castellan, N.J., 1988. *Nonparametric Statistics for the Behavioral Sciences*, second ed. McGraw-Hill, New York.
- Suggett, D.J., Stambler, N., Prášil, O., Kolber, Z., Quigg, A., Dominguez, E., Zohary, T., Berman, T., Iluz, D., Levitan, O., Lawson, T., Meeder, E., Lazar, B., Bar-Zeev, E., Medova, H., Berman-Frank, I., 2009. Nitrogen and phosphorus limitation of oceanic microbial growth during spring in the Gulf of Aqaba. *Aquat. Microb. Ecol.* 56, 227–239.
- Takamura, N., Zhu, X.B., Yang, H.Q., Ye, L., Hong, F., Miura, T., 1992. High biomass and production of picoplankton in a Chinese integrated fish culture pond. *Hydrobiologia* 237, 15–23.
- Verhoeven, K.J.F., Simonsen, K.L., McIntyre, L.M., 2005. Implementing false discovery rate control: increasing your power. *Oikos* 108, 643–647.
- Wolf-Vecht, A., Paldor, N., Brenner, N., 1992. Hydrographic indications of advection/convection effects in the Gulf of Eilat. *Deep-Sea Res.* 39, 1393–1401.
- Wu, R.S.S., Lam, K.S., MacKay, D.W., Lau, T.C., Yam, V., 1994. Impact of marine fish farming on water quality and bottom sediment: a case study of the sub-tropical environment. *Mar. Environ. Res.* 38, 115–145.
- Wu, R.S.S., 1995. The environmental impact of marine fish culture: towards a sustainable future. *Mar. Pollut. Bull.* 31, 159–166.
- Yahel, G., Post, A.F., Fabricius, K., Marie, D., Vulot, D., Genin, A., 1998. Phytoplankton distribution and grazing near coral reefs. *Limnol. Oceanogr.* 43, 551–563.